J Electr Eng Technol Vol. 8, No. 6: 1365-1370, 2013
http://dx.doi.org/10.5370/JEET.2013.8.6.1365

ISSN(Print) 1975-0102
ISSN(Online) 2093-7423

Numerical Calculations and Analyses in Diagonal Type Magnetohydrodynamic Generator

Le Chi Kien†

Abstract – This paper examines the effects of magnetic induction attenuation on current distribution in the exit regions of the Faraday-type, non-equilibrium plasma Magnetohydrodynamic (MHD) generator by numerical calculation using cesium-seeded helium. Calculations show that reasonable magnetic induction attenuation creates a very uniform current distribution near the exit region of generator channel. Furthermore, it was determined that the current distribution in the middle part of generator is negligible, and the output electrodes can be used without large ballast resistors. In addition, the inside resistance of the exit region and the current concentration at the exit electrode edges, both decrease with the attenuation of magnetic flux density. The author illustrates that the exit electrodes of the diagonal Faraday-type, non-equilibrium plasma MHD generator should be arranged in the attenuation region of the magnetic induction, in order to improve the electrical parameters of the generator.

Keywords: Numerical calculation, MHD generator, Diagonal type, Ballast resistance, Two-dimensional analysis

1. Introduction

The quasi one-dimensional MHD theory [1-2] tells us that performance characteristics of a diagonal-type, non-equilibrium MHD generator are similar to the performance characteristics of a Faraday-type MHD generator. However, the quasi one-dimensional MHD theory is only relevant when talking about the boundary conditions of the working gas plasma, and does not accurately reflect the spatial non-uniformity effects in a cross-section of the generator's channel. Moreover, so-called end effects arise in the exit regions of the MHD generators, degrading the total electrical performance.

Through numerical analysis, the author has investigated the electrical performance in the central part of the diagonal type non-equilibrium MHD generator channel as described in [3].

In addition, while the end effects in the Faraday-type generator have been analyzed in fair detail [4-6], the end effects in the diagonal-type require further analysis [7-9]. Thus, the author has investigated influences of the output electrodes' arrangement and the attenuation of the magnetic induction along the generator channel on the current, as well as potential distributions near the entrance and exist exit of the diagonal-type MHD channel when physical quantities in the channel are assumed to be uniform. The author's examinations demonstrate that the variation of the arrangements of output electrodes has little effect on current distribution, etc. [10]

In this paper the author studies the end effects in the diagonal-type, non-equilibrium MHD generator through numerical analysis. Section 2, introduces basic equations and boundary and subsidiary conditions, and then shows the configurations of gas velocity and applied magnetic induction adopted throughout the paper. In section 3, numerical calculations are made, to investigate the effect of the magnetic induction attenuation on current and potential distributions, internal resistance, etc., in the exit regions of the generator.

2. Basic Equations

2.1 Basic equations for current distribution

In the analysis of end effects in a diagonal-type MHD generator, the following assumptions are made: 1) the electric quantities, such as the current, electric field etc., vary with x and y, where x and y are the coordinates as shown in Fig. 1, and 2) the gas velocity and temperature depend only on y according to (9) and (10) which will be presented later, and 3) the pressure is kept constant.

In order to evaluate the current distribution in the generator channel, the author introduce the conventional stream function Ψ defined by:

$$J_x = \partial \Psi / \partial y, J_y = -\partial \Psi / \partial x \quad (1)$$

where J_x and J_y are the x and y components of current

† Corresponding Author: Faculty of Electrical and Electronics Engineering, Ho Chi Minh City-University of Technical Education, Vietnam. (kienlc@hcmute.edu.vn)
Received: February 17, 2013; Accepted: May 27, 2013

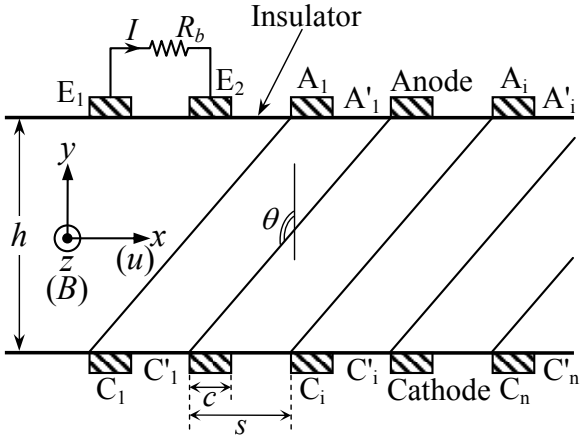

Fig. 1. Coordinate system and generator channel geometry

density, and the z component J_z is assumed not to exist.

Then, it is assumed that the magnetic induction and the gas velocity have only the z component B and the x component u, respectively. From the Maxwell and the generalized Ohm's law Eqs. (1) and (2) in [3], the following partial differential equation can be derived:

$$\nabla^2\Psi + P\partial\Psi/\partial x + Q\partial\Psi/\partial y = R \tag{2}$$

where,

$$\left.\begin{aligned} P &= \sigma/\varepsilon\{\partial(\varepsilon/\sigma)/\partial x - \partial(\beta/\sigma)/\partial y\} \\ Q &= \sigma/\varepsilon\{\partial(\varepsilon/\sigma)/\partial y + \partial(\beta/\sigma)/\partial x\} \\ R &= \sigma/\varepsilon\{-\partial(\partial p_e/\partial y/en_e)/\partial x + \\ &\quad +\partial(\partial p_e/\partial x/en_e)/\partial y + \\ &\quad +u\partial B/\partial x\} \\ \varepsilon &= 1+\beta\beta_i \end{aligned}\right\} \tag{3}$$

in which e is the electron charge, $p_e=n_ekT_e$ is the electron partial pressure, n_e is the electron density, k is the Boltzmann constant, T_e is the electron temperature, β is the Hall parameter for electron, β_i is the Hall parameter for an ion, and σ the scalar electrical conductivity of the plasma. In addition, $\sigma=\mu n_e e$, $\beta=eB/n_em_eQc_e$ are explained in detail in [3], where μ is electron mobility, m_e is electron mass, Q is the collision cross section, and c_e is the velocity of individual electron.

2.2 Boundary and subsidiary conditions

First, the boundary conditions on the electrode surfaces is defined as:

$$E_x = 0 \tag{4}$$

where, E_x is the x component of the electric field.

The boundary condition on the insulating wall surface is defined as:

$$J_y = 0 \tag{5}$$

Using (1), these conditions (4) and (5) are transformed to:

$$\varepsilon\partial\Psi/\partial y - \beta\partial\Psi/\partial x - \sigma\partial p_e/\partial x/en_e = 0 \tag{4′}$$

$$\Psi = const \tag{5′}$$

Next, in the diagonal-type generator, the potential difference between the anode A_i and cathode C_i must be zero as shown in Fig. 1. Therefore, the first subsidiary condition is obtained as:

$$V_i = -\int_{A_i}^{C_i} \boldsymbol{E}\mathrm{ds} = 0\ ,\ i=1, 2, \ldots, \mathrm{n} \tag{6}$$

where, $\boldsymbol{E}$ is the electric field intensity vector, ds is the line element vector of an optional integral path from A_i to C_i, and V_i is the potential difference between A_i and C_i.

As the load current I runs through an arbitrary surface S_i, it crosses the insulating wall surfaces A'_i and C'_i, the second subsidiary condition is written as

$$\int_{S_i} \boldsymbol{J}\mathrm{dS} = I\ ,\ i=1, 2, \ldots, \mathrm{n} \tag{7}$$

where dS is the element vector of the surface S_i.

Finally, let us assume that the electric quantities vary periodically in the period of the electrode pitch s along the gas flow behind the n-th electrode pair A_n and C_n. Then the condition for the current density $\boldsymbol{J}(x)$ is given by

$$\boldsymbol{J}(x+s) = \boldsymbol{J}(x) \tag{8}$$

By (1, 8) is transformed into

$$\Psi(x+s) = \Psi(x) + I_y^{(n)} \tag{8′}$$

where $I_y^{(n)}$ is the current flowing into A_n.

The current distributions in the diagonal type generator can be found by numerically solving (2) under the conditions (4′)~(7) and (8′) (see section 3).

2.3 Calculation of potential

With the obtained numerical solution of Ψ, (2) can be solved numerically using conditions (4′)~(7) and (8′), and the electric field $\boldsymbol{E}$ at the optional point can be evaluated using (1) and the generalized Ohm's law. Then, the potential at any point can be calculated by the numerical line integration of $\boldsymbol{E}$ along an arbitrary integral path from a reference point to the point in consideration.

2.4 Gas velocity and temperature distributions

As assumed in section 2, the velocity u has only the x component u, and u and T vary only in the y-direction according to the following relation [11]

$$u/u_0 = \{4y/h(1-y/h)\}^m \quad (9)$$

$$(T-T_w)/(T_0-T_w) = \{4y/h(1-y/h)\}^n \quad (10)$$

where, h is the channel height, u_0 is the gas temperature and T_0 is the velocity at the center of flow, namely $y=h/2$ and T_w is the wall temperature.

2.5 Configuration of applied magnetic induction

For effective use of the applied magnetic flux density B, the MHD generator channel should be arranged in the attenuation region of B. Thus, in order to investigate the influence of the configuration of B on the current distribution in the exit regions of the diagonal type generator, the intensity of B is assumed to be constant in the central region and decreases linearly from the left edge of the j-th electrode in the exit regions of the generator. In this this numerical analysis, the author assumes the six configurations of B as plotted in Fig. 2, where g is the gradient of B and j=5.

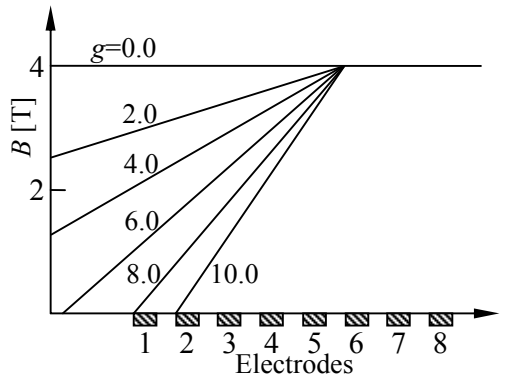

Fig. 2. Configuration of applied magnetic induction

3. Numerical Method for Subsidiary Conditions

In a diagonal generator, the solution of (3) is required to satisfy the two subsidiary conditions (6) and (7). From (1) and (7), the author can derive the following equation:

$$\Psi_i^{A'} - \Psi_i^{C'} = I/w,\ i=1, 2,\ldots, \mathrm{n} \quad (11)$$

where $\Psi_i^{A'}$ and $\Psi_i^{C'}$ are the values of Ψ on the insulating wall surfaces A_i' and C_i' respectively, and w is the channel width in the z direction.

First, if the values of I and w are assumed and $\Psi_i^{A'}$ are given plausible values, the values of $\Psi_i^{C'}$ are decided by (11). When (2) is digitally solved with these values of $\Psi_i^{A'}$ and $\Psi_i^{C'}$, and using the appropriately assumed values of u, σ and β, the author can obtain the numerical solution of Ψ. By applying the solution to (1) and the generalized Ohm's law, the author can find the values of E_x and E_y. Furthermore, by substituting the values of E_x and E_y into the integral in (6), the author can decide the value of V_i. Then the value of V_i obtained is not necessarily equal to zero.

Let us consider the resistance between the electrodes A_i and C_i

$$R_i' = h/\{\langle\sigma\rangle_i cw\cos(\pi-\theta)\},\ i=1, 2,\ldots, \mathrm{n} \quad (12)$$

where h, c and θ are the channel height, the electrode width and the angle of inclination to the y axis of the lines joining the equipotential electrodes, respectively, and the author assume that an imaginary current defined by

$$I_i = V_i/R_i',\ i=1, 2,\ldots, \mathrm{n} \quad (13)$$

flows through the resistance R_i'. To make V_i zero, it is needed to flow the inverse current $-I_i$ through R_i. Then it is required to increase by $-I_i$ the value of $w(\Psi_{i+1}^{A'} - \Psi_i^{A'})$, which gives the current running into the anode A_i.

Again beginning with the new modified values of $\Psi_i^{A'}$, the author must repeat the above mentioned calculation process. When V_i becomes adequately small after the many repetitions of the above mentioned process, at last the author can obtain the satisfactory numerical solution of Ψ.

In connection, the other parts of numerical calculation processes are explained in [12].

4. Numerical Calculation

4.1 Numerical conditions

Numerical analysis is carried out for the diagonal type MHD generator with the cesium seeded helium in non-equilibrium ionization using the following parameters:

$$\left.\begin{aligned} &h=0.2, s=0.1, w=0.1, c=0.06\mathrm{m} \\ &T_0=1800\mathrm{K}, T_w=1600\mathrm{K}, p=5\mathrm{atm} \\ &u_0=2000\mathrm{m/s}, m=n=1/7, B_0=4\,or\,5\mathrm{T} \\ &\delta=5, \varepsilon_s=0.3\% \end{aligned}\right\} \quad (14)$$

where ε_s is the seed fraction of C_s, B_0 is the magnetic induction in the central region of generator channel, and δ is the collision loss factor. These conditions are assumed with respect to a generator of the pilot plant [13]. The load current I is assumed to flow equally into two output

electrodes E_1 and E_2 through a ballast resistance R_b defined by (see Fig. 1)

$$R_b = -\int_{E_1}^{E_2} \boldsymbol{E}\mathrm{d}s/(I/2) \tag{15}$$

4.2 Calculation results

In Figs. 3(a)~(c), the current distributions are plotted in the case of g=0, 6 and 10T/m, respectively, B_0=4T and I=70A, where the contour interval of current streamlines is 1/20 of the load current I. In the figures, $\langle J\rangle_{el}$= 0.583A/cm^2, $\langle\sigma\rangle$=1.84 mho/m, $\langle\beta\rangle$=2.01 and β_{crit}=2.48, where $\langle J\rangle_{el}$ is the average current density on the output electrodes, $\langle\sigma\rangle$ and $\langle\beta\rangle$ are the average electrical conductivity and Hall parameter in the center of flow, respectively, and β_{crit} is the critical Hall parameter [14].

Fig. 3(a) shows that the current concentration at the edges of the output electrodes is very intensive when B does not attenuate. On the other hand, Figs. 3(b) and (c) indicate that the concentration weakens as the attenuation of B increases, since β becomes small in the area suffering a spatial reduction of B. Also it is seen that the current flowing into a diagonally connected electrode pair reduces with an increasing gradient of magnetic induction in the entrance region of channel. For instance, the currents of about 60, 25 and 15% of I flow into C, when g=0, 6 and 10T/m, respectively. Also the figures denote that the eddy current is not induced when the output electrodes are disposed in the region of the attenuating magnetic induction [5], and that arranging the output electrodes within the attenuation region of B does not have a great influence on the current distribution in the central part of generator channel.

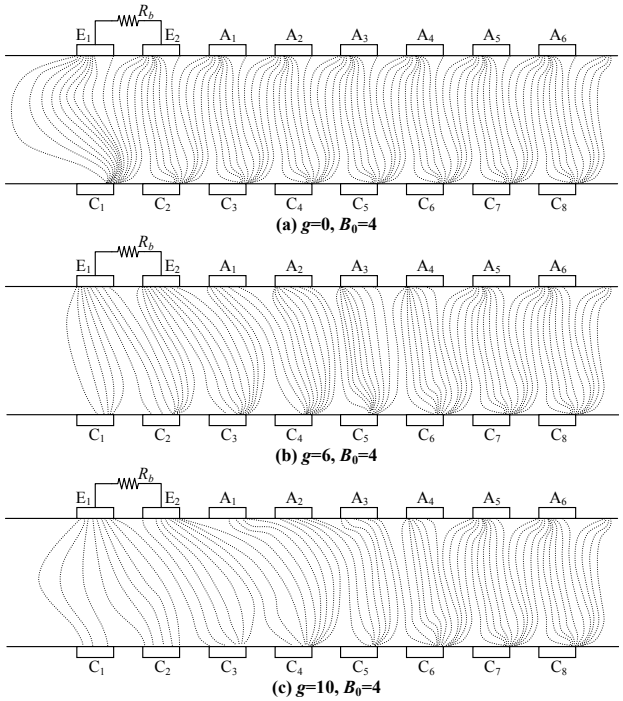

Fig. 3. Current distributions

Next, Fig. 4 shows the variation of the potential difference between the electrode pairs A_1-C_1~A_8-C_8 and the electrode E_1. From the figures it is seen that the relatively large potential difference arises between the two output electrodes E_1 and E_2 when B does not attenuate, namely g=0. On the other hand, the potential difference become smaller as g becomes larger, it almost vanishes for g=6, and the inverse difference appears for g>7. Also Fig. 4 demonstrates that the potential differences in the central part of generator channel are influenced little by the decrease of the magnetic induction.

Next, for estimation of the end effects of the generator, the author evaluates the internal resistance R_i of the exit regions and the grade of the current concentration on the output electrodes given by the relations

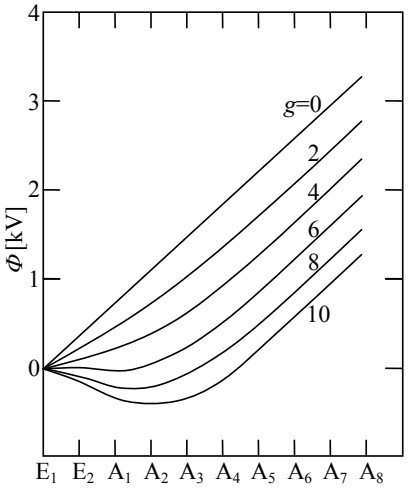

Fig. 4. Variation of potential difference for B_0=4

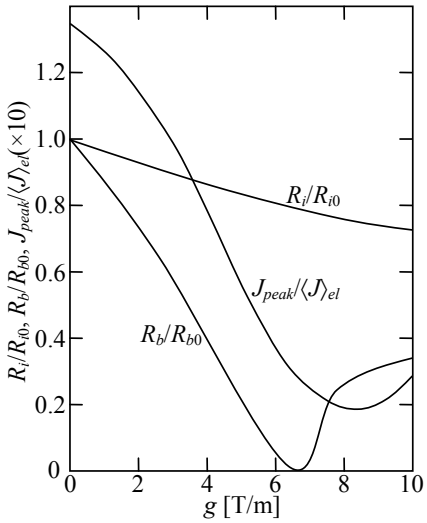

Fig. 5. Influence of g on R_i/R_{i0}, R_b/R_{b0} and $J_{peak}/\langle J\rangle_{el}$ when B_0=4

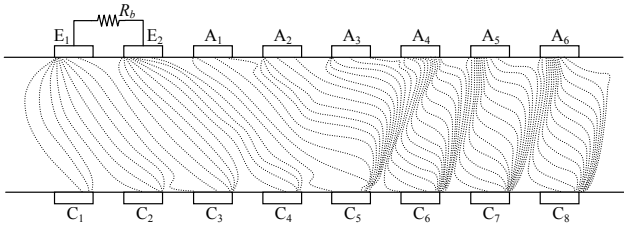

Fig. 6. Current distribution for g=6 and B_0=5

$$R_i = (V_0 - V)/I \tag{16}$$

$$J_{peak}/\langle J\rangle_{el} \geq 1 \tag{17}$$

where V_0 and V are no-load and load potential difference between the output electrode E_1 and the n-th electrode, respectively, and J_{peak} is the maximum current density on the output electrodes. In this connection, $J_{peak}/\langle J\rangle_{el}$=1 means the state of no current concentration and $J_{peak}/\langle J\rangle_{el}$>>1 does the intensive current concentration at an electrode edge.

Now Fig. 5 shows the variations of R_i/R_{i0}, R_b/R_{b0} and $J_{peak}/\langle J\rangle_{el}$ by g, where R_{i0} and R_{b0} are R_i and R_b for g=0, respectively. From the figure, it is seen that R_i decreases with g, for instance the value of R_i for g=6.0 becomes about 80% of the one of R_{i0}, and that $J_{peak}/\langle J\rangle_{el}$ decreases from g=0 to 8T/m, reaches the minimum value 1.90 and increases again. This fact shows that the current concentration at the edges of the output electrodes is almost diminished when g=8T/m. Accordingly, arranging the output electrodes in the attenuation area of the magnetic flux density is useful to guard the output electrodes. Also Fig. 5 tells that R_b/R_{b0} decreases with g, becomes almost zero for g=6.5 and then increases with g. Therefore, it is shown that many output electrodes will require large ballast resistors when B does not attenuate or exceeds 8, but they can be used without large ballast resistors in the range of g=6~7T/m.

In Fig. 6, the current distribution is plotted when g=6T/m, B_0=5T and I=150A, $\langle J\rangle_{el}$=1.25A/cm^2, $\langle\sigma\rangle$=2.85 mho/m, $\langle\beta\rangle$=2.48 and β_{crit}=1.90. The figure indicates that the streamer is induced in the central part of generator, while the current distribution becomes successively uniform as B attenuates along the generator channel and the current concentration is almost swept away near the output electrodes. This demonstrates that arranging the output electrodes within the attenuating region of B is effective for the case where the streamer is generated in the central region of generator channel, too.

5. Conclusions

The main conclusions derived from the above described numerical calculation are as follows:

A suitable distribution of the magnetic flux density can make the current distribution very uniform near the exit region of generator channel, both when the streamer is not induced and when it is induced in the central region.

Disposing the output electrodes within the attenuation area of magnetic flux density has little influence on the current distribution in the central part of generator channel.

When the output electrodes are disposed in the region with a suitably reduced magnetic flux density, the potential difference and the ballast resistance between two output electrodes become very small. Accordingly it is thought that many output electrodes can be used without large ballast resistors.

The internal resistance in the exit region of the generator channel decreases as the magnetic flux density attenuates.

The current concentration at the edges of output electrodes can be fairly eliminated by attenuating magnetic flux density.

As mentioned above, it is made clear that the output electrodes of the diagonal type non-equilibrium plasma MHD generator should be arranged in the region of the attenuating magnetic flux density, since arranging them in the region of the decreasing magnetic flux density become useful for the improvement of the electrical performance of the generator.

References

[1] H. Yamaguchi, Y. Hisazumi, H. Asano, H. Morita, T. Hori, T. Matsumoto, T. Abiko, “A New Heat Supply System of Cogeneration for the Local Community”, JSME Journal of Power and Energy Systems, Vol.2, No.3, pp.1085-1095, 2008.

[2] Y. Hamada, K. Amazawa, S. Murakawa, H. Kitayama, M. Nabeshima, H. Takata, “Study on Operation Characteristics and Performance Evaluation of Residential Combined Heat and Power System”, JSER 27th International Conference on Energy, Economy, and Environment, 7-1, pp.453-458, 2011.

[3] S. Takeshitaa, C. Buttapeng, N. Harada, “Characteristics of plasma produced by MHD technology and its application to propulsion systems”, Vacuum, Vol. 84, Iss. 5, pp. 685-688, 2009.

[4] V.A. Bityurin, “MHD Electrical Power Generation in a T-Layer Plasma Flow”, IEEE Transactions on Plasma Science, Vol. 28, Iss. 3, pp. 1020-1028, 2000

[5] S.M. Aithal, “Shape Optimization of a MHD Generator Based on Pressure Drop and Power Output Constraints”, International Journal of Thermal Sciences, Vol.47, Iss.6, pp.778-786, 2008.

[6] S.M. Aithal, “Characteristics of Optimum Power Extraction in a MHD Generator with Subsonic and Supersonic Inlets”, Energy Conversion and Management, Vol.50, Iss.3, pp.765-771, 2009.

[7] M. Anwari, N. Sakamoto, T. Hardianto, J. Kondo, N. Harada, “Numerical Analysis of Magnetohydrodynamic Accelerator Performance with Diagonal

Electrode Connection", Energy Conversion and Management, Vol. 47, Iss. 13-14, pp. 1857-1867, 2006.
[8] Motoo Ishikawa, Fumiki Inui, Juro Umoto, "Fault Analysis of a Diagonal Type MHD Generator Controlled with Local Control Circuit", Energy Conversion and Management, Vol. 40, Iss. 3, pp. 249-260, 1999.
[9] B.S. Bhadoria, A. Chandra, "Transient Analysis of Proposed Indian MHD Channel", Energy Conversion and Management, Vol. 42, Iss. 8, pp. 963-966, 2001.
[10] Y. Inui, H. Ito, T. Ishida, "Two Dimensional Simulation of Closed Cycle Disk MHD Generator Considering Nozzle and Diffuser", Energy Conversion and Management, Vol. 45, Iss. 13-14, pp. 1993-2004, 2004.
[11] Y. Gelfgat, J. Krūminš, B.Q. Li, "Effects of System Parameters on MHD Flows in Rotating Magnetic Fields", Journal of Crystal Growth, Vol. 210, Iss. 4, pp. 788-796, 2000.
[12] E. M. Braun, R. R. Mitchell, A. Nozawa, D. R. Wilson, F. K. Lu, J. C. Dutton, "Electromagnetic Boundary Layer Flow Control Facility Development Using Conductive Nanoparticle Seeding", 46th Aerospace Sciences Meeting and Exhibit, AIAA Paper 2008-1396, 2008.
[13] Lingen Chen, Jianzheng Gong, Fengrui Sun, Chih Wu, "Heat Transfer Effect on the Performance of MHD Power Plant", Energy Conversion and Management, Vol. 43, Iss. 15, pp. 2085-2095, 2002.
[14] E. Sawaya, N. Ghaddar, F. Chaaban, "Evaluation of the Hall Parameter of Electrolyte Solutions in Thermosyphonic MHD Flow", International Journal of Engineering Science, Vol. 40, Iss. 18, pp. 2041-2056, 2002.

Le Chi Kien He received B.S degree in Electrical Engineering from HCMC-University of Technical Education, Vietnam in 1997. He received his M.S. and Ph.D. degree from Nagaoka University of Technology, Japan in 2002 and 2005. Since 2005, he is lecturer at HCMC-University of Technical Education, Faculty of Electrical and Electronics Engineering. His research interests are high efficiency power generation systems, Magnetohydrodynamics and combined systems.